

## Article

# A Time Series Decomposition-Based Interpretable Electricity Price Forecasting Method

Yuanke Cu <sup>1</sup>, Kaishu Wang <sup>2,3,4</sup> , Lechen Zhang <sup>5</sup>, Zixuan Liu <sup>2,3,4</sup> , Yixuan Liu <sup>2,3,4</sup>  and Li Mo <sup>2,3,4,\*</sup> 

<sup>1</sup> Guizhou Qianyuan Electric Power Co., Ltd., Guiyang 550002, China; yuankecu@outlook.com

<sup>2</sup> School of Civil and Hydraulic Engineering, Huazhong University of Science and Technology, Wuhan 430074, China; m202271627@hust.edu.cn (K.W.); zixuan\_liu@hust.edu.cn (Z.L.); m202171608@hust.edu.cn (Y.L.)

<sup>3</sup> Hubei Key Laboratory of Digital River Basin Science and Technology, Huazhong University of Science and Technology, Wuhan 430074, China

<sup>4</sup> Institute of Water Resources and Hydropower, Huazhong University of Science and Technology, Wuhan 430074, China

<sup>5</sup> China Electric Power Research Institute Co., Ltd., Hangzhou 310030, China; lechenz@outlook.com

\* Correspondence: moli@hust.edu.cn

**Abstract:** Electricity price forecasting is of significant practical importance, and improving prediction accuracy has become a key area of focus. Although substantial progress has been made in electricity price forecasting research, the unique characteristics of the electricity market make prices highly sensitive to even minor market changes. This results in prices exhibiting long-term trends while also experiencing sharp fluctuations due to sudden events, often leading to extreme values. Furthermore, most current models are “black-box” models, lacking transparency and interpretability. These unique features make electricity price forecasting particularly complex and challenging. This paper introduces a forecasting framework that incorporates the Seasonal Trend decomposition using Loess (STL), Gated Recurrent Unit (GRU), Light Gradient Boosting Machine (LightGBM), and Shapley Additive Explanations (SHAPs) and applies it to forecasting in the electricity markets of the United States and Australia. The proposed forecasting framework significantly improves prediction accuracy compared to nine other baseline models, especially in terms of *RMSE* and  $R^2$  metrics, while also providing clear insights into the factors influencing the forecasts. On the U.S. dataset, the *RMSE* of this framework is 12.7% lower than that of the second-best model, while, on the Australian dataset, the *RMSE* of the SLGSEF is 2.58% lower than that of the second-best model.



Received: 12 January 2025

Revised: 24 January 2025

Accepted: 29 January 2025

Published: 31 January 2025

**Citation:** Cu, Y.; Wang, K.; Zhang, L.; Liu, Z.; Liu, Y.; Mo, L. A Time Series Decomposition-Based Interpretable Electricity Price Forecasting Method. *Energies* **2025**, *18*, 664. <https://doi.org/10.3390/en18030664>

**Copyright:** © 2025 by the authors. Licensee MDPI, Basel, Switzerland. This article is an open access article distributed under the terms and conditions of the Creative Commons Attribution (CC BY) license (<https://creativecommons.org/licenses/by/4.0/>).

## 1. Introduction

As the marketization of electricity trading progresses, research on electricity prices has become a prominent area of focus [1]. The accurate forecasting of electricity prices is crucial for facilitating the rational and efficient dispatch of power systems, thereby ensuring the safe and reliable operation of power systems [2]. Various stakeholders in the electricity market, including power generators and electricity consumers, place considerable importance on price forecasting. Generators can use such forecasts to devise bidding strategies, while consumers rely on them to optimize production activities efficiently and reduce electricity costs [3]. Electricity price forecasting holds significant practical value in

real-world applications. Therefore, many scholars have conducted extensive research on electricity price forecasting using various modeling methods [4].

Existing electricity price forecasting methods can be categorized into statistical models and machine learning models. Statistical models include Autoregressive (AR) [5], Autoregressive Moving Average (ARMA) [6], and Autoregressive Integrated Moving Average (ARIMA) models [7], among others. These statistical models rely on the temporal relationships within the data for forecasting and are suitable for relatively stable datasets. However, electricity price data exhibit high levels of randomness and intermittency [8]. Traditional statistical models struggle to capture the volatility characteristics of electricity prices, leading to poor forecasting performance. As a result, machine learning models have become one of the key tools for electricity price forecasting [9].

Marcos et al. [10] developed various Machine Learning models, including the Linear Regression model (LR) [11], Random Forest (RF) [12], Long Short-Term Memory (LSTM) [13], and GRU, to forecast electricity prices in the Spanish market. Their results indicated that, for this dataset, the GRU network proved to be the most effective model for predicting electricity prices and modeling electricity consumption. Gokgoz and Filiz conducted short-term electricity price forecasting using the Stacked Denoising Autoencoder (SDA) model, focusing on both online hourly forecasting and day-ahead forecasting. The results show that the SDA model is capable of accurately forecasting electricity prices [14]. Although machine learning algorithms have shown promising performance in electricity price forecasting, their effectiveness is hindered by the complexity of electricity prices. These algorithms are highly dependent on parameter selection, and a single forecasting model struggles to capture the various features of electricity price fluctuations [15]. Current research tends to integrate different individual models into a hybrid forecasting model to improve prediction efficiency [16]. Loizidis et al. studied the price distribution in the German and Finnish electricity markets and proposed a novel method combining Extreme Learning Machine with Bootstrap intervals for day-ahead electricity price forecasting. The results show that this method performs better in terms of forecasting accuracy and computational efficiency, effectively addressing market uncertainty and negative price phenomena [17]. Pourdaryaei et al. proposed an electricity price forecasting method based on multi-head self-attention and Convolutional Neural Networks (CNNs), combined with mutual information and neural networks (NNs) for feature selection to improve forecasting accuracy [18]. Laitkos et al. used a hybrid CNN-GRU model and Transformer models for electricity price forecasting. The results show that the hybrid CNN-GRU model achieved the best prediction accuracy [19].

To reduce the impact of non-stationary characteristics in the sequence on forecasting accuracy, most existing studies employ data decomposition techniques to achieve denoising. Wendong Yang et al. proposed an adaptive parameter-based variational mode decomposition technique to provide ideal data preprocessing results, thereby improving the forecasting accuracy of the model [20]. Jaseena K et al. proposed a wind speed forecasting framework based on data decomposition techniques and bidirectional long short-term memory (BiDLSTM) networks. By combining methods such as wavelet transform and empirical wavelet transform for denoising and separately forecasting low-frequency and high-frequency signals, they demonstrated that using appropriate data decomposition algorithms can further enhance the forecasting accuracy of the model [21].

Although significant progress has been made in electricity price forecasting research, the unique characteristics of the electricity market make it highly sensitive to even small market changes. This results in prices exhibiting long-term trends while also experiencing sharp fluctuations due to sudden events, often leading to extreme values. Furthermore, most current models are “black-box” models, lacking transparency and interpretability.

These unique features make electricity price forecasting particularly complex and challenging [22,23].

This paper proposes an interpretable forecasting framework based on time series decomposition (STL-LightGBM-GRU-SHAP explainable framework, SLGSEF). The contributions of this model are as follows:

- The Seasonal Trend decomposition procedure based on Loess (STL) [24] is employed to extract temporal features from complex electricity price data. This serves as a crucial input for the model, significantly enhancing prediction quality and accuracy through effective data decomposition and model selection.
- The GRU model captures long-term dependencies within the electricity price time series, while the Light Gradient Boosting Machine (LightGBM) [25] captures the impact of other features on electricity price fluctuations. By combining the two base models through an Error-Weighting method, the framework retains comprehensive and valuable information throughout the learning process.
- Shapley Additive Explanations (SHAPs) are used to analyze the contribution of each feature to the proposed predictive model's performance on specific tasks, thereby enhancing the interpretability of electricity price predictions. By comparing with classical electricity price forecasting models and incorporating Structural Equation Modeling (SEM), the predictive capability and reliability of the proposed framework are validated.

The rest of this paper is structured as follows: Section 2 describes the basic structure of the SLGSEF framework and the algorithm process; Section 3 introduces the principles of the underlying models; Section 4 compares the proposed framework with the prediction results of multiple underlying models and discusses the findings. Finally, Section 5 summarizes the current research results, limitations, and directions for future research.

## 2. Model Structure

The SLGSEF framework requires Python version 3.8 or higher. It depends on libraries including NumPy, Pandas, Matplotlib, Statsmodels, Sklearn, Shap, and Keras. For the SLGSEF framework, it is crucial to standardize raw data into a CSV format or generate a Pandas DataFrame using Python functions. The dataset should include electricity prices as well as features that are correlated with these prices, such as weather conditions and capacity. Additionally, it should incorporate lagged features obtained by applying lag transformations to the electricity prices.

The SLGSEF forecasting framework proposed in this paper comprises two components: prediction and interpretation. The framework is illustrated in Figure 1.

The specific steps are as follows:

### (1) Data Cleaning

The data cleaning process consists of three parts: missing value detection, outlier removal, and normalization. For outliers, they are first identified using the LOF algorithm, then replaced with missing values, and filled using linear interpolation. This algorithm is an outlier detection method based on density, which is used to identify anomalous data points in a dataset. By calculating the density ratio of each data point to its surrounding neighbors, it determines whether the current data point is an outlier. If the density of a sample data point is relatively lower than that of its neighboring data points, it is likely to be an outlier. To mitigate the impact of the dimensionality of multi-parameter time series on data analysis, the data are normalized. The normalization formula is as follows:

$$\bar{x} = \frac{x - x_{\min}}{x_{\max} - x_{\min}} \quad (1)$$

## (2) Feature Processing

Considering the short-term response to fluctuations in electricity prices and the long-term trend changes, lagged features of electricity prices are processed at multiple time scales with time intervals of 5 min, 1 h, 12 h, and 1 day. The lagged features are then merged with the raw dataset of electricity prices to form a new dataset. Pearson's correlation analysis, as well as Spearman's rank correlation analysis, was used to assess the correlation between the features and electricity prices and to select the relevant input variables.

## (3) STL Decomposition

Decompose the cleaned electricity price data into trend, seasonal, and residual components. The seasonal and residual components are then combined into a single variation component.

## (4) Model Training and Prediction

Use LightGBM and GRU to train and predict the trend and variation components obtained in the previous step, respectively. For LightGBM, a feature set is required as input, while GRU uses only historical electricity price data for training. The prediction results are combined using an inverse Error-Weighting method to produce the forecast values for the trend and variation components, which are then merged to obtain the final forecast value. The formula for the inverse Error-Weighting method is as follows:

$$\hat{f}_m = \omega_1 f_{1m} + \omega_2 f_{2m}, \quad m = 1, 2, \dots, n \quad (2)$$

$$\omega_1 = \frac{\varepsilon_2}{\varepsilon_1 + \varepsilon_2} \quad (3)$$

$$\omega_2 = \frac{\varepsilon_1}{\varepsilon_1 + \varepsilon_2} \quad (4)$$

In the formula,  $\omega_i$  represents the weighting coefficient, and  $f_{1m}$  and  $f_{2m}$  are the prediction results from the LSTM and LightGBM models, respectively.  $\varepsilon_1$  and  $\varepsilon_2$  denote the prediction errors from LSTM and LightGBM, and  $\hat{f}_m$  is the final forecasted value and the number of samples in the test set.

## (5) Evaluation of Prediction Results

The model evaluation metrics used to assess the prediction results include the Mean Absolute Error (MAE), Root Mean Squared Error (RMSE), Coefficient of Determination ( $R^2$ ), Mean Absolute Percentage Error (MAPE), Mean Relative Error (MRE), and Integral of Absolute Error (IAE). The calculation formulas are as follows:

$$MAE = \frac{1}{n} \sum_{m=1}^n |f_m - \hat{f}_m| \quad (5)$$

$$RMSE = \sqrt{\frac{1}{n} \sum_{m=1}^n (f_m - \hat{f}_m)^2} \quad (6)$$

$$R^2 = 1 - \frac{\sum_{m=1}^n (f_m - \hat{f}_m)^2}{\sum_{m=1}^n (f_m - \bar{f}_m)^2} \quad (7)$$

$$MAPE = \frac{1}{n} \sum_{i=1}^n \left| \frac{f_m - \hat{f}_m}{f_m} \right| \times 100 \quad (8)$$

$$MRE = \frac{1}{n} \sum_{i=1}^n \left| \frac{f_m - \hat{f}_m}{f_m} \right| \quad (9)$$

$$IAE = \int_0^t |f_m - \bar{f}_m| dt \quad (10)$$

In the formula,  $f_m$  represents the actual value, and  $\bar{f}_m$  is the mean of all actual values.

#### (6) Interpretability Analysis

Construct an SEM (Structural Equation Modeling) model to analyze the correlation between historical electricity prices and various features. Additionally, establish SHAP (SHapley Additive exPlanation) models for the GRU and LightGBM models used in Step 3 to assess the impact of each feature on the prediction outcomes.

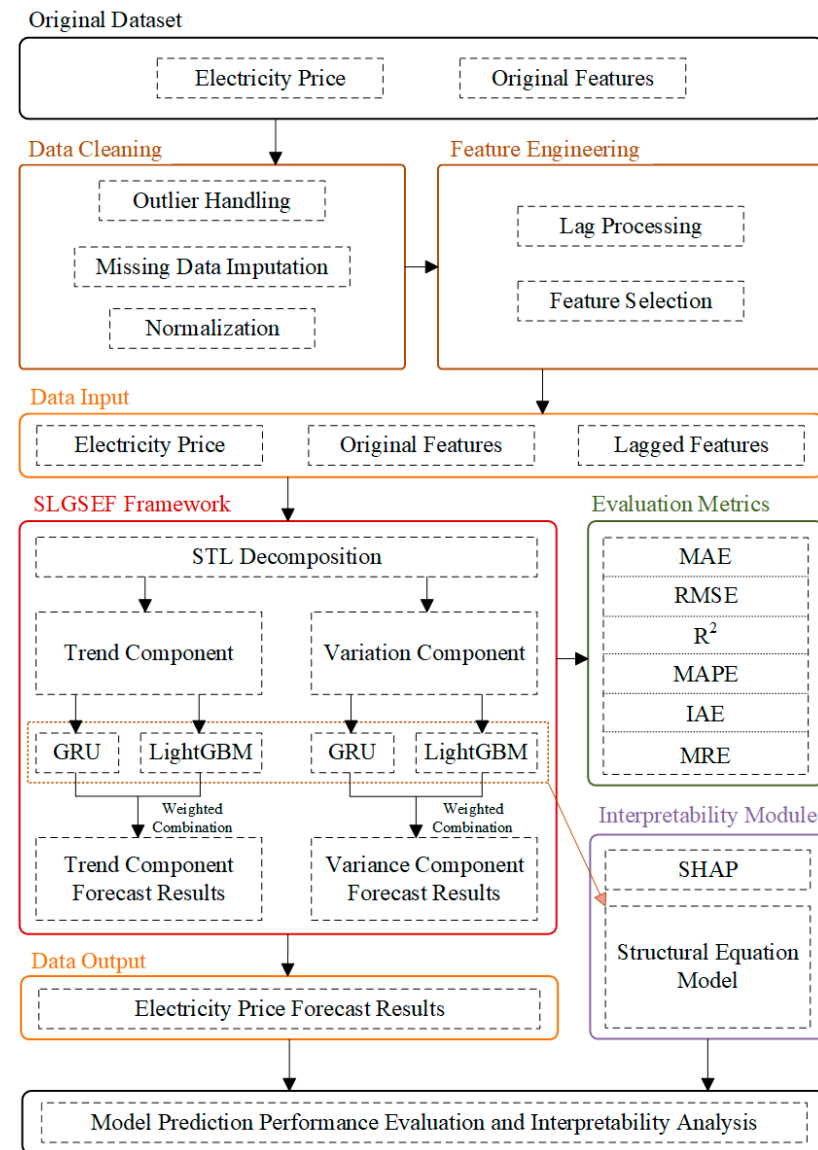


**Figure 1.** SLGSEF forecasting framework diagram.

### 3. Model Methodology

#### 3.1. STL Decomposition

STL (Seasonal Trend decomposition using Loess) decomposition applies locally weighted regression (Loess) to fit the cyclical trend and seasonal components of a time series, breaking it down into trend, seasonal, and residual components. STL decomposition can handle various forms of seasonal variations, but it also has limitations. When dealing with highly irregular or noisy time series data, it may encounter restrictions, failing to

capture long-term dependencies or dynamic changes in the data [26]. This method offers two types of decomposition models: additive and multiplicative [27]. In this paper, we use the additive model for decomposition, represented by the following equation:

$$H_t = T_t + S_t + R_t \quad (11)$$

In the equation,  $H_t$  represents the time series data,  $T_t$  is the trend component, and  $S_t$  is the seasonal component and the residual component.

### 3.2. GRU Model

The GRU can be regarded as a variant of the LSTM model, adopting a similar gating mechanism to capture long-term dependencies. However, there are notable differences between the two. Unlike LSTM, the GRU has a simpler structure, merging the forget gate and the input gate into a single gating mechanism called the “update gate”. By reducing one gate and the associated matrix multiplication operations, the GRU can significantly save time when processing large-scale training data [28]. The structure of the GRU is illustrated in Figure 2.

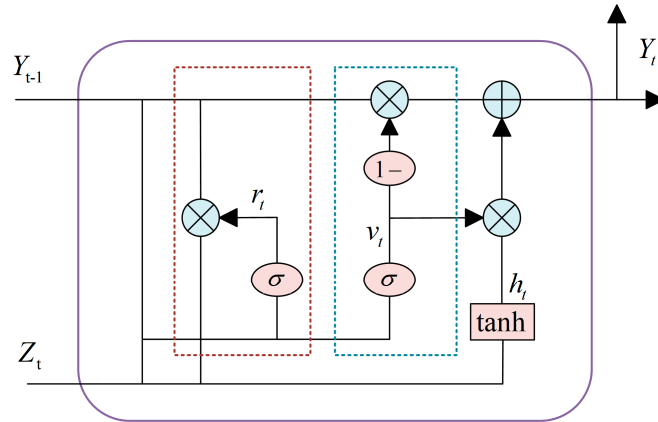


**Figure 2.** GRU cell structure diagram.

The mathematical description is as follows:

$$v_t = \sigma(W_v \cdot [Y_{t-1}, Z_t] + b_v) \quad (12)$$

$$r_t = \sigma(W_r \cdot [Y_{t-1}, Z_t] + b_r) \quad (13)$$

$$h_t = \tanh(W_h \cdot [r_t \cdot Y_{t-1}, Z_t] + b_h) \quad (14)$$

$$Y_t = (1 - v_t) \cdot Y_{t-1} + v_t \cdot h_t \quad (15)$$

In the formula,  $Z_t$  represents the input at the current time step,  $Y_{t-1}$  denotes the output from the previous time step, and  $Y_t$  is the output at the current time step.

### 3.3. LightGBM Model

The LightGBM, an enhanced framework based on decision tree algorithms, was developed by Microsoft and released in 2017 [29]. It is characterized by fast training speed, low memory usage, and reduced communication costs during parallel learning. Key features of the LightGBM include a decision tree algorithm that incorporates Gradient-based One-Side Sampling (GOSS), Exclusive Feature Bundling (EFB) [30], as well as a histogram-based approach and a leaf-wise growth strategy with depth constraints. Unlike most decision tree algorithms, which typically employ a level-wise growth approach, the LightGBM adopts a leaf-wise growth strategy with depth limitations [31]. In this strategy,

the algorithm selects the leaf node with the highest split gain and proceeds iteratively, as illustrated in Figure 3.

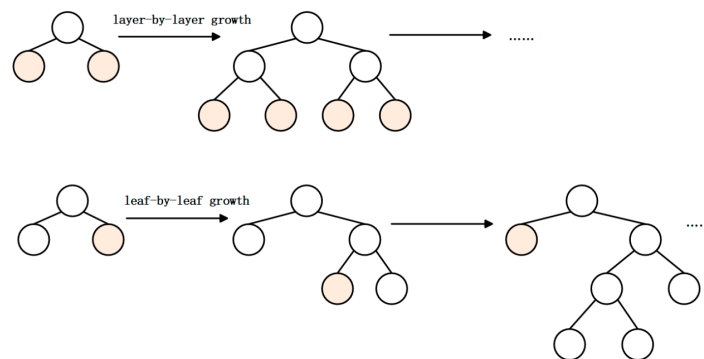


**Figure 3.** Decision tree growth strategy diagram.

Compared to the level-wise growth strategy, the leaf-wise growth approach can reduce larger errors and achieve higher accuracy, thereby offering solutions for various problems.

### 3.4. Interpretability Analysis Methods

#### 3.4.1. SHAP Model

Proposed by Lundberg et al. in 2017 [32], the core concept of SHAPs (Shapley Additive exPlanations) is to calculate the marginal contribution of each feature to the model's output, thereby interpreting the “black-box model” from both global and local perspectives. SHAP can analyze the contribution of each feature to the model's predictions, identifying the most critical features for electricity price forecasting. This process helps in eliminating unnecessary input features, simplifying the model structure, and reducing the risk of overfitting. Additionally, it provides concrete directions for model optimization, such as enhancing predictive accuracy by adjusting feature weights or incorporating feature interactions.

$$f(x_{ij}) = mc_{ij}w_j + \dots + mc_{ij}w_n \quad (16)$$

In the formula,  $x_{ij}$  represents the feature of the sample,  $mc_{ij}$  denotes the marginal contribution of the feature,  $w_j$  represents the edge weight, and  $f(x_{ij})$  is the SHAP value for the sample. If  $f(x_{ij})$  is greater than 0, it indicates that the feature has increased the prediction value, playing a positive role. Conversely, if  $f(x_{ij})$  is less than 0, it implies that the feature has decreased the prediction value, thus exerting a negative effect.

#### 3.4.2. SEM Model

The Structural Equation Modeling (SEM) model is an analytical framework used to construct and validate complex relationships between variables. This model can reveal the interconnections among multiple variables and introduce latent variables [33], thereby providing a clearer understanding of the intrinsic influence mechanisms and causal relationships between variables.

## 4. Case Study Analysis

### 4.1. Data Sources

In this experiment, we selected 8928 frequency regulation price data points from the United States PJM frequency regulation ancillary service market, recorded at 5 min intervals from 1 July to 31 July 2023. Additionally, we used 8064 settlement price data points from the Queensland spot market in Australia, recorded at 5 min intervals from 1 February to 1 March 2023.

The United States PJM frequency regulation dataset includes not only the Market Clearing Price (MCP) but also the Capability Clearing Price (CCP) and Performance Clearing Price (PCP). The Australian spot market dataset contains the Recommended Retail Price (RRP) for electricity, as well as the Total Demand. Besides the original features of each dataset, we applied lag processing to the electricity prices in both datasets at intervals of 5 min, 1 h, 12 h, and 1 day to generate lagged features. These lagged features were then combined with the original features to create a new, enriched feature set.

#### 4.2. Correlation Analysis

Correlation analysis was performed on the U.S. dataset and the Australian dataset. Tables 1 and 2 present the Pearson correlation coefficients for the U.S. and Australian datasets, respectively, while Tables 3 and 4 display the Spearman correlation coefficients for the U.S. and Australian datasets, respectively.

**Table 1.** Pearson correlation coefficient table (U.S.).

	MCP	CCP	PCP	mcp_5m	mcp_1h	mcp_12h	mcp_1d
MCP	1	0.232 **	0.243 **	-0.127 **	0.228 **	0.202 **	-0.057 **

\*\* Correlation is significant at the 0.01 level (two-tailed).

**Table 2.** Pearson correlation coefficient table (Australia).

	RRP	TOTALDEMAND	RRP_5m	RRP_1h	RRP_12h	RRP_1d
RRP	1	0.578 **	0.687 **	0.687 **	0.685 **	-0.048 **

\*\* Correlation is significant at the 0.01 level (two-tailed).

**Table 3.** Spearman correlation coefficient table (U.S.).

	MCP	CCP	PCP	mcp_5m	mcp_1h	mcp_12h	mcp_1d
MCP	1.000	0.255 **	0.277 **	-0.208 **	0.253 **	0.254 **	0.023 *

\* Correlation is significant at the 0.05 level (two-tailed), \*\* Correlation is significant at the 0.01 level (two-tailed).

**Table 4.** Spearman correlation coefficient table (Australia).

	RRP	TOTALDEMAND	RRP_5m	RRP_1h	RRP_12h	RRP_1d
RRP	1.000	0.609 **	0.674 **	0.675 **	0.679 **	-0.069 **

\*\* Correlation is significant at the 0.01 level (two-tailed).

As can be seen from the table, all features exhibit significant correlation with electricity prices. Therefore, the above features are selected as inputs for the LightGBM model.

#### 4.3. STL Decomposition Results

Given that both datasets have a 5 min interval, we selected a 1 h period to decompose the electricity prices. The residuals from the decomposition conform to a normal distribution with a mean of zero, indicating that the STL method effectively decomposed the electricity prices into trend, seasonal, and residual components. The seasonal and residual components were subsequently combined to form the variation component.

The decomposition results of the electricity prices for both datasets are shown in Figure 4.

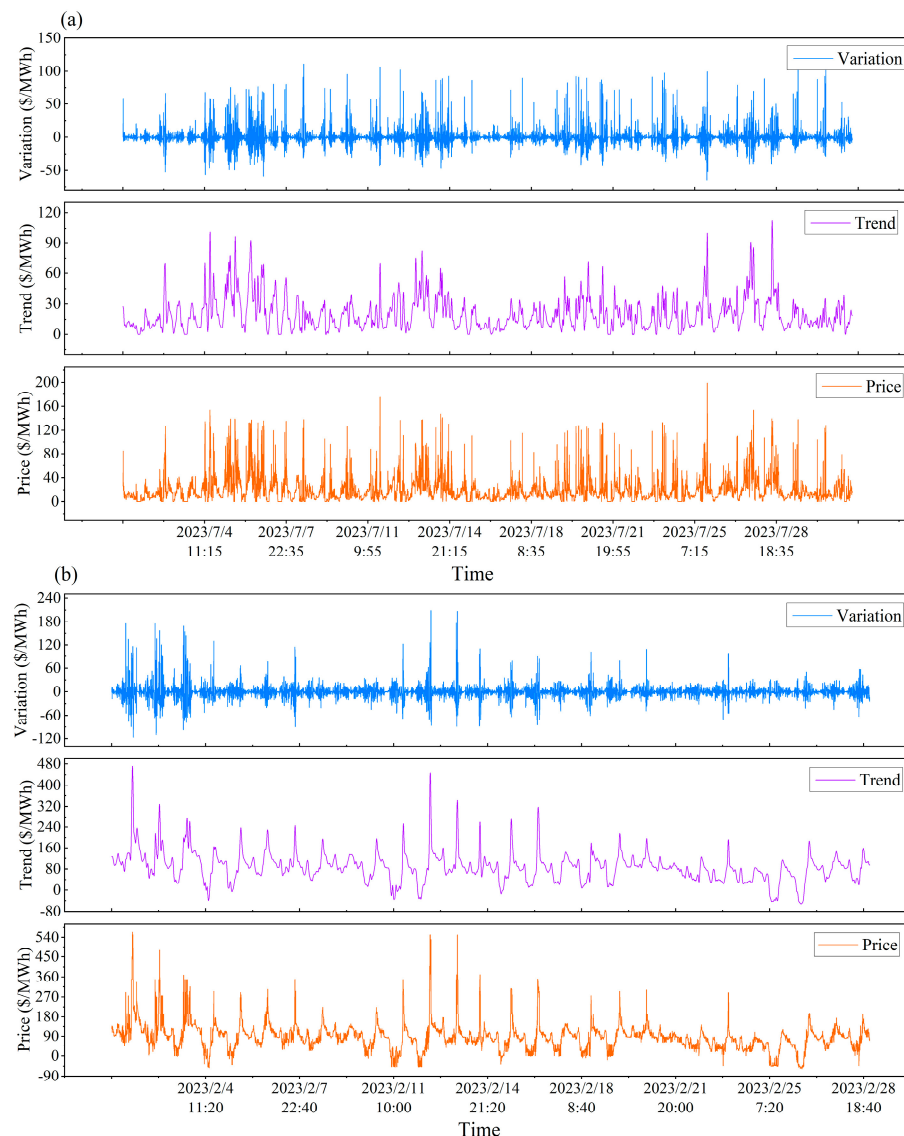


**Figure 4.** Decomposition result diagram: (a) the decomposition results for the United States PJM frequency regulation market prices, and (b) the decomposition results for the spot prices in Queensland, Australia.

#### 4.4. Evaluation and Analysis of Prediction Results

This study validated the predictive performance of the proposed SLGSEF forecasting framework. We employed the SLGSEF model along with comparison models, including the LightGBM-GRU weighted ensemble model (referred to as the LG model), the STL-GRU model (referred to as the SG model), the STL-LightGBM model (referred to as the SL model), as well as independent GRU and LightGBM models. Additionally, models such as the XGBoost model, Support Vector Machine model (referred to SVM), Random Forest model (referred to RF), and Long Short-Term Memory model (referred to LSTM) were also included. The comparison between the predicted results of different models and the actual values is shown in Figure 5.

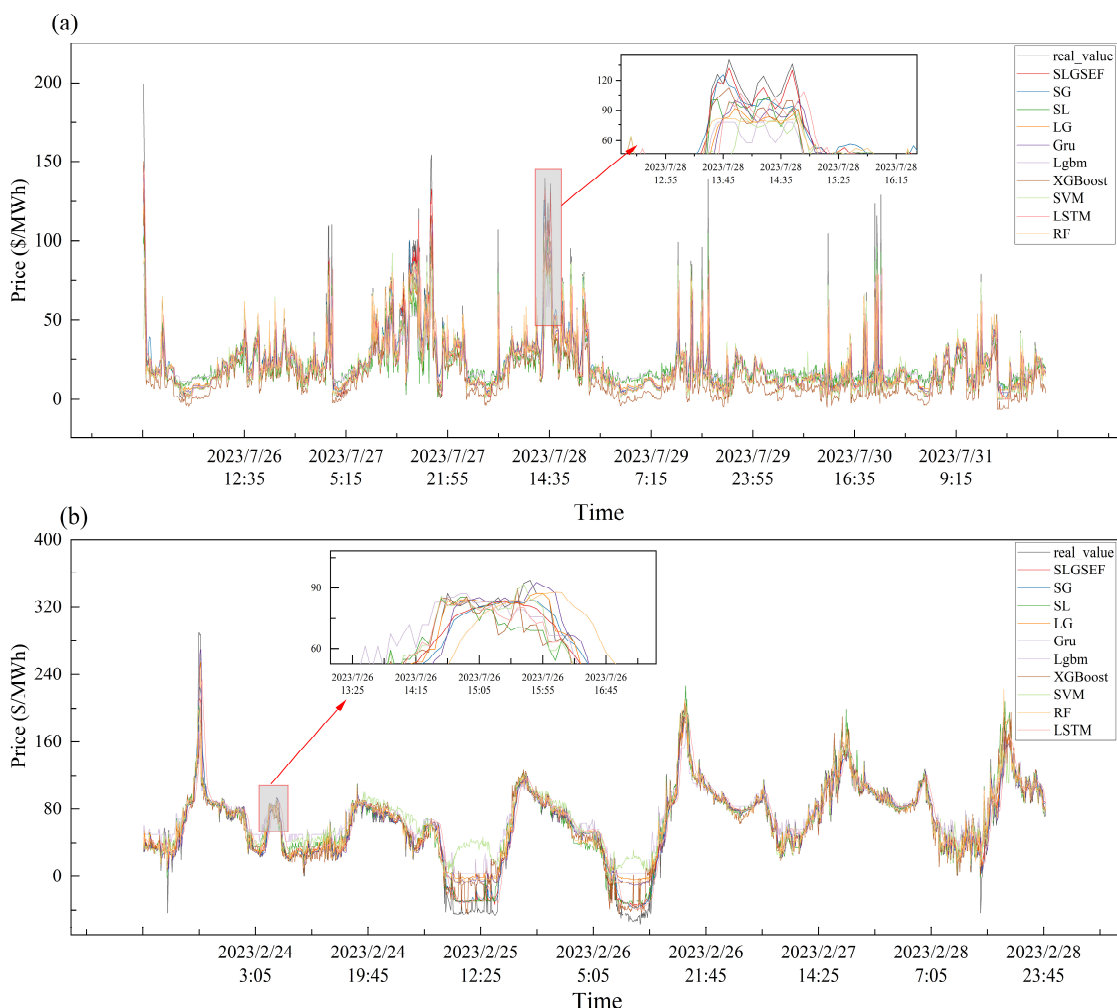


**Figure 5.** Model forecasting result comparison diagram: (a) the prediction results for the United States PJM frequency regulation market prices, and (b) the results for the Queensland spot market prices in Australia.

To present the prediction results more clearly, the predicted outcomes are plotted as scatter plots. The figure below shows the scatter plots of the prediction results for each model. As shown in Figure 6, the SLGSEF model exhibits the best predictive performance.

To further investigate the predictive performance of different models, we use the Mean Absolute Error (MAE), Root Mean Squared Error (RMSE), Coefficient of Determination ( $R^2$ ), Mean Absolute Percentage Error (MAPE), Mean Relative Error (MRE), and Integral of Absolute Error (IAE) as evaluation metrics. Table 5 shows a comparison of the evaluation results for various prediction models on the U.S. PJM market dataset.

As the data show, the SLGSEF performs excellently across all metrics, especially in the RMSE and  $R^2$ , where it demonstrates a significant advantage over other models. Specifically, the RMSE of the SLGSEF is 6.95, which is notably lower than the next best model, RF, with an RMSE of 7.96, representing a 12.7% reduction in error and a marked improvement in prediction accuracy. Additionally, the SLGSEF achieves an  $R^2$  of 0.90, a 3.45% improvement over the RF model. Although the RF model has an advantage in the MAPE and IAE, these metrics only have localized significance in specific error calculations. From an overall prediction performance perspective, the SLGSEF remains the most outstanding. For the MAE, the SLGSEF achieves the best value at 3.72, further validating its stability and reliability.

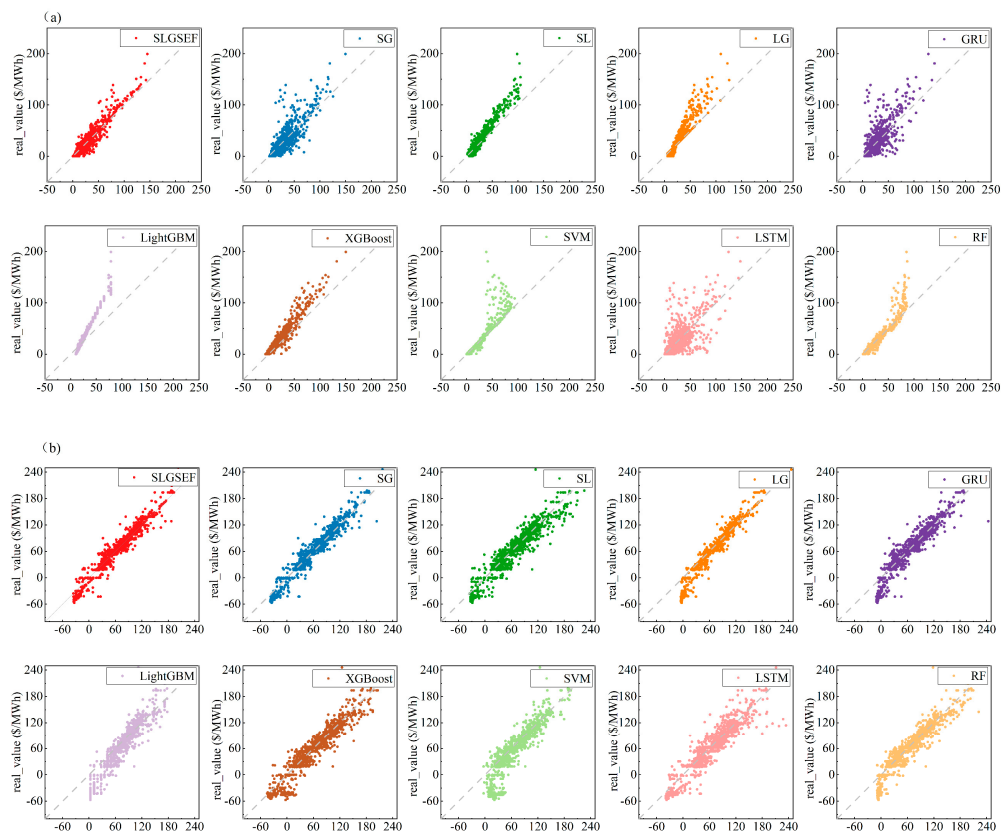


**Figure 6.** Scatter plot of model prediction results: (a) the prediction results for the United States PJM frequency regulation market prices, and (b) the results for the Queensland spot market prices in Australia.

**Table 5.** Model forecasting result evaluation table (U.S.).

Model	United States					
	RMSE	MAE	R <sup>2</sup>	MAPE	IAE	MRE
SLGSEF	6.95	3.72	0.90	28.07	6602.92	28.07
LG	10.02	4.70	0.80	39.82	8345.47	39.82
SL	9.29	6.31	0.83	61.10	11,213.81	61.10
LightGBM	11.63	7.34	0.73	69.93	13,011.46	69.93
SG	11.26	5.93	0.75	44.22	10,523.23	44.22
GRU	13.34	6.67	0.65	45.30	11,834.47	45.30
XGBoost	10.30	7.94	0.79	57.48	14,100.23	57.48
SVM	10.10	2.18	0.80	10.94	3870.02	10.94
RF	7.96	2.78	0.87	20.23	4934.18	20.23
LSTM	15.61	8.04	0.52	53.68	14,283.12	53.68

Table 6 shows a comparison of the evaluation results for various prediction models on the Australian dataset.

On the Australian dataset, the SLGSEF outperforms other models in all metrics or is very close to the next best model. In terms of the RMSE and R<sup>2</sup>, the SLGSEF stands out the most. Specifically, the RMSE of the SLGSEF is 11.35, which is 2.58% lower than the next best model, SG, indicating smaller prediction errors. For the R<sup>2</sup>, the SLGSEF achieves 0.95, a 1.06% improvement over SG, further demonstrating the fitting ability of the SLGSEF. In terms of the MAE, SLGSEF's value is 7.23, a 4.87% reduction in error compared to the SG model, indicating more accurate predictions. Although the SLGSEF is slightly higher than SG in the MAPE and MRE, the difference is very small, and, in IAE, the SLGSEF has

the lowest value. Therefore, the predictive ability of the SLGSEF can still be considered superior to that of the next best model, SG.

**Table 6.** Model forecasting result evaluation table (Australia).

Model	Australia					
	RMSE	MAE	R <sup>2</sup>	MAPE	IAE	MRE
SLGSEF	11.35	7.23	0.95	335.38	11,596.93	335.38
LG	15.85	8.23	0.90	335.79	13,195.53	335.79
SL	15.42	10.75	0.90	496.39	17,230.93	496.39
LightGBM	22.50	15.70	0.80	950.16	25,179.92	950.16
SG	11.65	7.60	0.94	329.04	12,184.14	329.04
GRU	16.58	10.49	0.88	274.26	16,826.75	274.26
XGBoost	17.18	11.19	0.88	421.91	17,935.55	421.91
SVM	25.63	15.52	0.74	727.13	24,875.21	727.13
RF	17.69	11.64	0.87	405.04	18,657.32	405.04
LSTM	18.32	12.06	0.86	747.09	19,326.66	747.09

This notable performance enhancement not only demonstrates the superiority of the SLGSEF model in terms of predictive accuracy but also highlights its robust capacity for handling complex time series data. Additionally, the SLGSEF model achieved  $R^2$  values close to one across both datasets, indicating a high degree of fit and explanatory power, which allows it to accurately capture the characteristics and trends of the data. This implies that the SLGSEF model is capable not only of making precise numerical predictions but also of faithfully reflecting the actual distribution of the data.

Figure 7 presents a comparison of the model evaluation metrics. From the comparison of these metrics, it can be observed that models optimized through STL decomposition generally outperform those without this optimization. Specifically, on the United States PJM frequency regulation dataset, the SLGSEF model showed a reduction in the RMSE and MAE by 31% and 21%, respectively, compared to the LG model. On the Australian Queensland spot market dataset, the reductions were 28% for the RMSE and 12% for the MAE. This indicates that, by decomposing the time series into distinct components with STL decomposition and modeling each component separately, the model can better capture the fluctuations in electricity prices, thereby effectively improving the prediction accuracy.

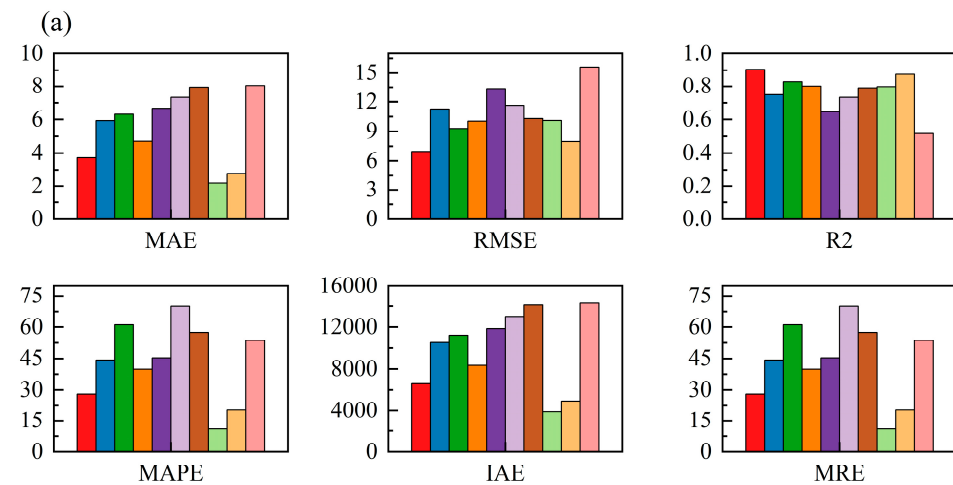


**Figure 7.** Cont.

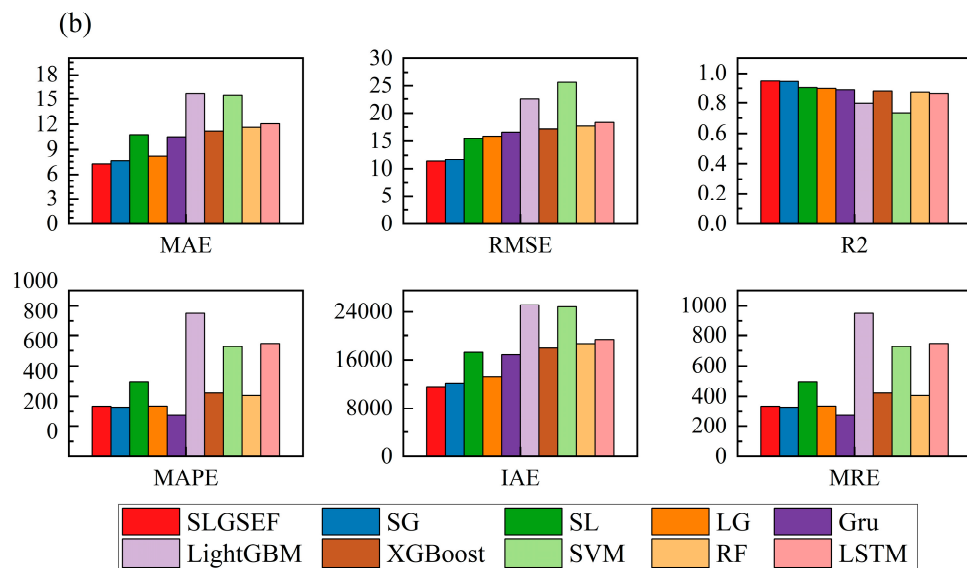


**Figure 7.** Model evaluation metric comparison diagram: (a) the model prediction evaluation metrics for the PJM market in the United States, and (b) the model prediction evaluation metrics for the Australian market.

#### 4.5. Interpretability Analysis

##### 4.5.1. Feature Impact Analysis with SEM

To thoroughly examine the influence of various features on prediction outcomes, this study constructs SEM models for two datasets from the United States and Australia. These models approach the analysis from three perspectives: trend components, variation components, and original electricity prices, to assess the impact of each feature. In this section, two latent variables are designed: lagged features and original features. Figure 8 illustrates the SEM model's structure and the path coefficients among variables.

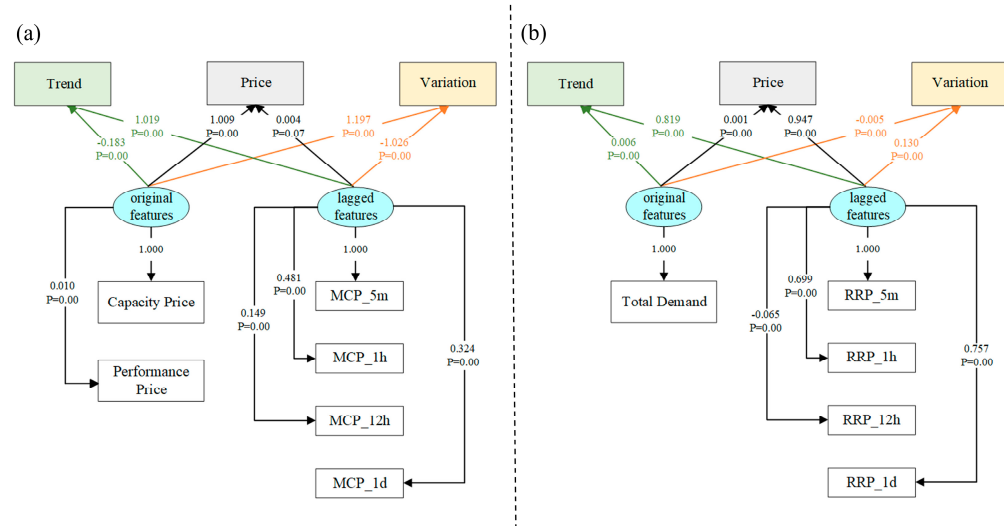


**Figure 8.** SEM structural and path coefficient diagram ( $p = 0.00$  indicates  $p < 0.001$ ): (a) the PJM frequency regulation market in the United States, and (b) the spot market in Queensland, Australia.

Analyzing the PJM frequency regulation market in the United States, from the perspective of absolute path coefficients, the impact of lagged features on the original electricity price (0.004) is nearly zero, which is significantly smaller than the impact of other features on it (1.009). In contrast, the trend component is more influenced by lagged features (1.019) compared to the influence of other features on it (0.183). For the variation com-

ponent, the effect of lagged features (1.026) is slightly smaller than that of other features (1.197), but this difference is not substantial. Observing the path coefficient variations across different features, the influence of lagged features on the original electricity price is minimal, nearly approaching zero. The proportion of the lagged feature influence within the trend component (85%) is markedly higher than its proportion within the variation component (46%).

Analyzing the Australian spot market from the perspective of absolute path coefficients, the influence of lagged features on the original electricity price, trend component, and variation component is significantly greater than that of other features. Examining the path coefficient variations across different features, the original electricity price is almost entirely influenced by lagged features, with an impact proportion approaching 100%. The influence proportion of lagged features within the trend component (99%) is notably higher than within the variation component (96%).

#### 4.5.2. SHAP Model Feature Contribution Analysis

In this section, based on the proposed SLGSEF forecasting framework, the SHAP model is introduced to conduct a comprehensive interpretability analysis of electricity price predictions for the LightGBM and GRU modules. This analysis covers three aspects—trend component, variation component, and original electricity price—across datasets from the United States and Australia. Figure 9 presents the SHAP feature importance diagrams for the LightGBM module.

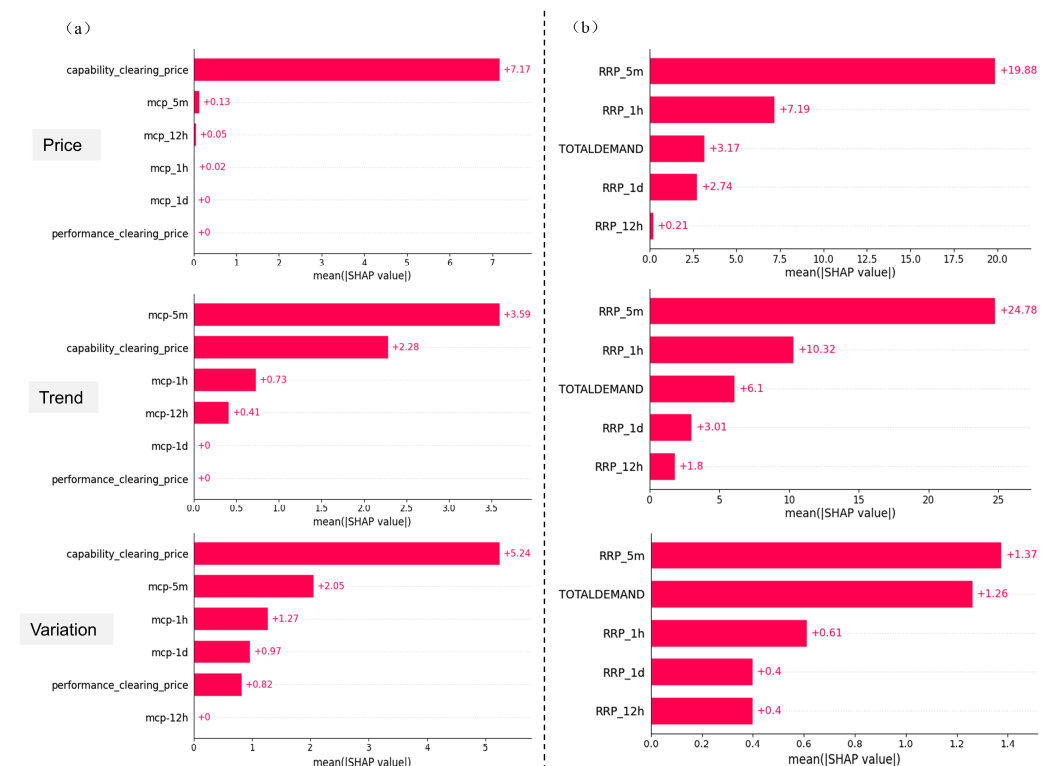


**Figure 9.** LightGBM module SHAP feature importance diagram: (a) the PJM frequency regulation market in the United States, and (b) the spot market in Queensland, Australia.

In analyzing the PJM frequency regulation market in the United States, it is evident that the trend component, variation component, and original electricity price show varying sensitivities to the input features. From the SHAP contribution values, for the original electricity price, other features contribute significantly more to the prediction outcome (7.17) compared to lagged features (0.2). Conversely, for the trend component, the contribution

of lagged features (4.73) is much greater than that of other features (2.28). Regarding the variation component, the contribution of other features (6.06) slightly exceeds that of lagged features (4.29). Examining the SHAP value variations across different features, the contribution proportion of lagged features to the original electricity price is minimal (3%), whereas, for the trend component, the contribution proportion of lagged features (67%) is higher than that for the variation component (41%). This indicates that, within the United States dataset, after the series undergoes STL decomposition, the model can account not only for the original features but also for the influence of lagged features during prediction. This insight reveals the rationale behind the improvement in prediction accuracy.

In analyzing the spot market in Queensland, Australia, SHAP contribution values indicate that, for the original electricity price, trend component, and variation component, lagged features contribute more to the prediction outcome than other features. Examining the SHAP value variations across different features, the original electricity price shows the highest contribution proportion from lagged features (90%), with the trend component also significantly influenced by lagged features (87%), which is notably higher than for the variation component (69%). This suggests that, for Australian electricity prices, STL decomposition allows the model to better account for the combined impact of both lagged and original features, thereby enhancing prediction accuracy.

To compare the feature contribution results obtained from the SEM model and the SHAP model, we use lagged features as an example and plot the influence ratios on electricity prices, trend components, and variation components for two datasets in Figure 10.

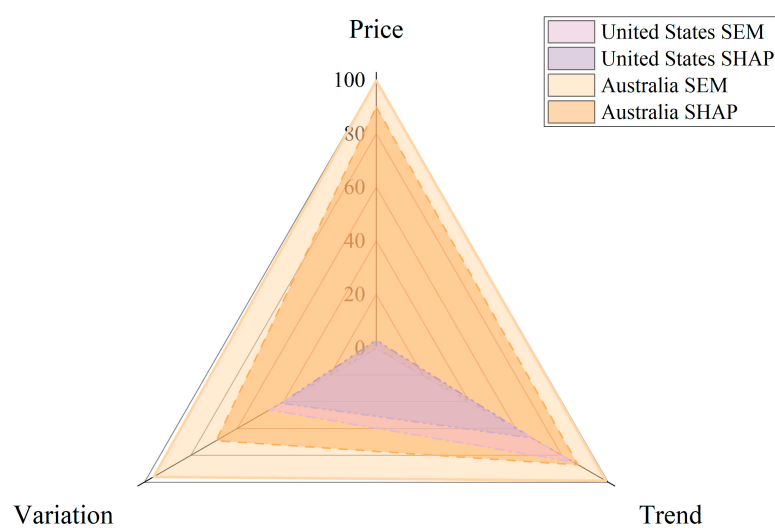


**Figure 10.** Lagged feature impact proportion diagram.

Analyzing Figure 9 reveals that, for the LightGBM module, the feature contribution results derived from SHAP analysis are consistent with the feature impact results obtained from the SEM model. In the case of the United States PJM frequency regulation market, lagged features have the greatest impact on the trend component, followed by the variation component, and exert almost no influence on electricity prices. For the Queensland spot market in Australia, lagged features primarily impact the original electricity price, followed by the trend component and the variation component.

Figure 11 presents the SHAP feature importance plot for the GRU module. Since no feature variables were input into the GRU model during training and prediction, this section analyzes the impact of time steps on the model's prediction results. The time step length for the model is set to 10, meaning the model considers 10 historical time steps when processing sequential data. When calculating SHAP values for sequential models, each time step can be treated as an independent sample, and SHAP values can be computed for

each time step. This approach helps in interpreting the influence of each time step's input on the model's output. Interpretability analysis is conducted for both the United States and Australian datasets from three perspectives: trend component, variation component, and original electricity price.

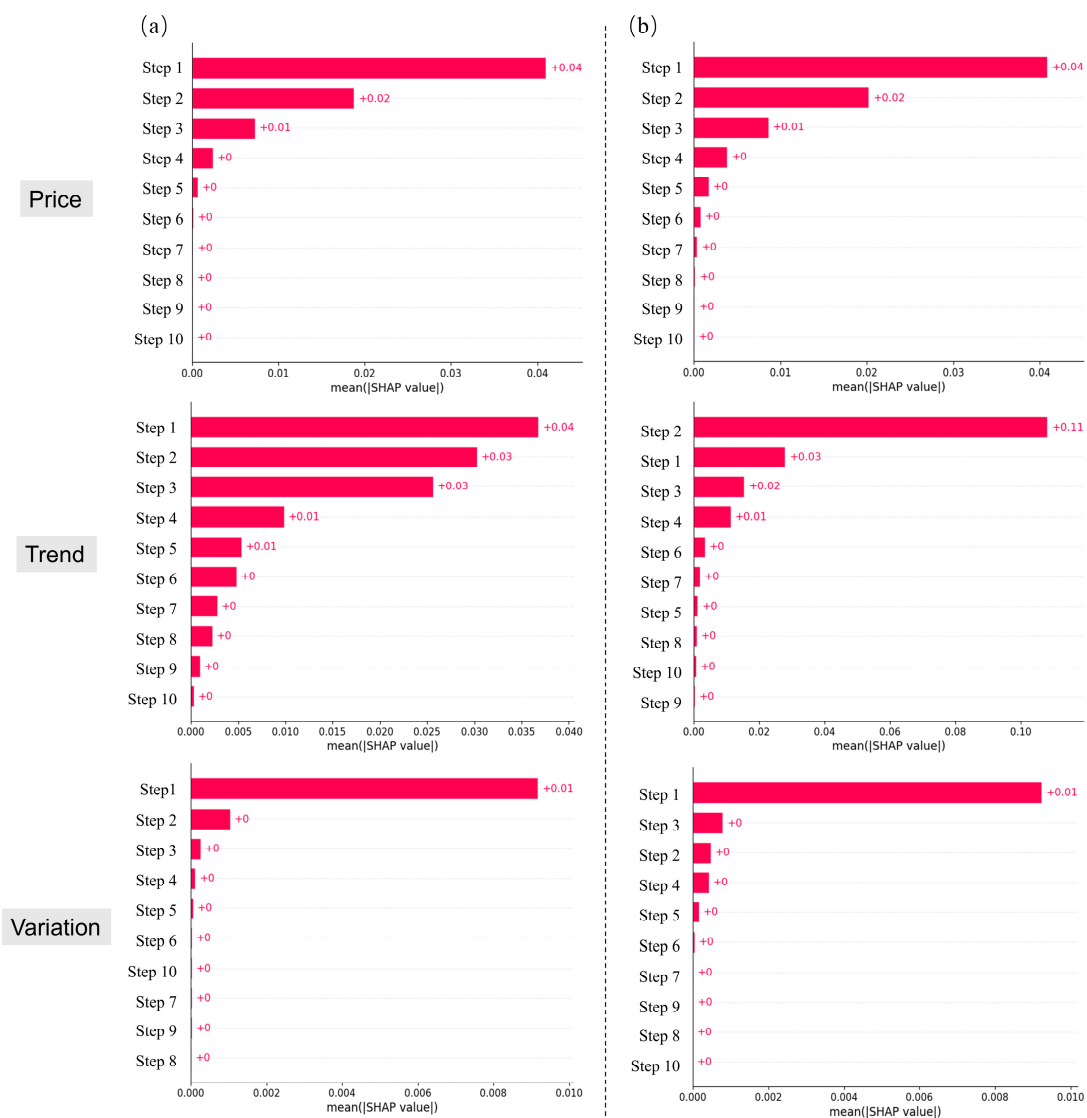


**Figure 11.** GRU module SHAP feature importance diagram: (a) the United States PJM frequency regulation market, and (b) the Queensland spot market in Australia.

It can be observed that, for both datasets, the GRU module only captures the influence of the most recent electricity prices when predicting the original electricity price and variation components. However, when predicting the trend component derived from STL decomposition, the GRU model can account for information from much earlier time points, thereby improving prediction accuracy. This indicates that STL decomposition effectively reduces noise, making the seasonality and periodicity of the trend component more pronounced. This enhancement allows the GRU to capture historical information more effectively, leading to improved accuracy.

## 5. Conclusions

This paper proposes an interpretable SLGSEF prediction framework and performs prediction and interpretative analysis on datasets from the United States and Australia. By

comparing with nine other commonly used baseline models, it is shown that the proposed framework achieves higher prediction accuracy on these datasets. Additionally, the proposed framework integrates SHAP and SEM models. The SHAP model provides insights into the contribution of each feature, while SEM helps analyze the causal relationships between these variables, thus enhancing the interpretability of the model and adding transparency to the black-box model. The main conclusions of this paper are as follows:

- The prediction accuracy of the SLGSEF significantly outperforms other baseline models. Particularly in terms of the  $RMSE$  and  $R^2$ , the SLGSEF framework demonstrates a clear advantage. On the U.S. dataset, the  $RMSE$  of the SLGSEF is 12.7% lower than that of the second-best model, and, on the Australian dataset, the  $RMSE$  of the SLGSEF is 2.58% lower than that of the second-best model. This not only proves the superior predictive accuracy of the SLGSEF model but also highlights its powerful ability to handle complex time series data. Furthermore, the  $R^2$  of the SLGSEF is close to one on both datasets, further validating the model's fitting capability.
- Models optimized using STL decomposition generally outperform non-optimized models, and the proposed SLGSEF prediction model exhibits the highest accuracy in the comparison, making it the best model. Specifically, on the U.S. PJM dataset, the SLGSEF reduces the  $RMSE$  and  $MAE$  by 31% and 21%, respectively, compared to the LG model. On the Australian dataset, the  $RMSE$  decreases by 28% and the  $MAE$  by 12%. This indicates that using STL decomposition to decompose the series effectively reduces noise, allowing the model to better capture the fluctuations and feature influences of each component, thereby improving prediction accuracy.

The SLGSEF framework has significant practical implications and can provide a more comprehensive direction for decision optimization. In electricity market forecasting, SHAP can identify key drivers of market behavior, while SEM can analyze the interactions between these factors and their overall impact on price fluctuations, thus offering more precise decision guidance for policymakers.

However, this study has certain limitations. The performance of the SLGSEF framework on long-term datasets requires further investigation. Nevertheless, the SLGSEF framework itself demonstrates good scalability, as its key components (STL decomposition, LightGBM, and GRU) are all capable of handling long-term time series data. For long-term datasets, STL decomposition can effectively extract long-term seasonal and trend features, making it suitable for long-term price data. The LightGBM, as an efficient gradient boosting method, can handle a large number of features in long-term datasets [34]. Its low memory consumption and fast training speed make it particularly efficient when processing long time series data. The GRU model is particularly well suited for capturing long-term dependencies [35,36]. Through hyperparameter tuning, the GRU can effectively learn patterns in long sequences.

Therefore, the SLGSEF framework already possesses the potential to handle long-term datasets and, with further optimization and adjustments, can be applied to larger-scale electricity price forecasting tasks with longer time spans.

**Author Contributions:** Conceptualization, L.M. and Y.C.; methodology, K.W.; formal analysis, K.W. and Y.L.; resources, L.Z.; data curation, Z.L.; writing—original draft, L.M. and K.W.; investigation, Y.C. and L.Z.; project administration, Y.C.; writing—review and editing, L.M. and Y.C.; visualization, L.Z.; validation, Z.L. and Y.L. All authors have read and agreed to the published version of the manuscript.

**Funding:** This research was funded by the National Natural Science Foundation of China (52379011) and the National Key Research and Development Program of China (2023YFC3209104).

**Data Availability Statement:** Data available upon request due to restrictions (e.g., privacy, legal or ethical reasons).

**Conflicts of Interest:** Yuanke Cu was employed by the company Guizhou Qianyuan Electric Power Co., Ltd.; Lechen Zhang was employed by the company China Electric Power Research Institute Co., Ltd., The remaining authors declare that the research was conducted in the absence of any commercial or financial relationships that could be construed as a potential conflict of interest.

## Abbreviations

The following abbreviations are used in this manuscript:

GRU	Gated Recurrent Unit
STL	Seasonal Trend decomposition using Loess
LightGBM	Light Gradient Boosting Machine
SHAP	Shapley Additive Explanations
SLGSEF	STL-LightGBM-GRU-SHAP explainable framework
LG	LightGBM-GRU weighted combination model
SG	STL-GRU model
SL	STL-LightGBM model
SEM	Structural Equation Modeling
MCP	Market Clearing Price
CCP	Capability Clearing Price
RRP	Recommended Retail Price
PCP	Performance Clearing Price
SVM	Support Vector Machine
XGBoost	eXtreme Gradient Boosting
RF	Random Forest
LSTM	Long Short-Term Memory

## References

1. Zhou, B.; Zhao, W.; Xuan, P.; Zhang, Y.; Yang, R.; Xu, Z. Research on the Key Influencing Factors of Electricity Spot Market Locational Marginal Price. *Guangdong Electr. Power* **2020**, *33*, 86–92.
2. Wang, W.; Ma, L.; Ming, Y.; Li, Z.; Wang, H.; Su, M.; Chen, Y.; Wang, N.; Chai, T. A Load-Marginal Price Joint Forecasting Method Based on Big Data. *Guangdong Electr. Power* **2021**, *34*, 10–17.
3. Feng, C.; Shao, L.; Wang, J.; Zhang, Y.; Wen, F. Short-term Load Forecasting of Distribution Transformer Supply Zones Based on Federated Model-Agnostic Meta Learning. *IEEE Trans. Power Syst.* **2024**, *40*, 31–45. [[CrossRef](#)]
4. Bâra, A.; Oprea, S.V.; Georgescu, I.A. Understanding electricity price evolution—day-ahead market competitiveness in Romania. *J. Bus. Econ. Manag.* **2023**, *24*, 221–244. [[CrossRef](#)]
5. Ofuji, K.; Kanemoto, S. Price forecasting of japan electric power exchange using time-varying AR model. In Proceedings of the 2007 International Conference on Intelligent Systems Applications to Power Systems, Kaohsiung, Taiwan, 5–8 November 2007; IEEE: New York, NY, USA, 2007; pp. 1–6.
6. Wang, R.; Yao, L.; Li, Y. A hybrid forecasting method for day-ahead electricity price based on GM (1, 1) and ARMA. In Proceedings of the 2009 IEEE International Conference on Grey Systems and Intelligent Services (GSIS 2009), Nanjing, China, 10–12 November 2009; IEEE: New York, NY, USA, 2009; pp. 577–581.
7. Contreras, J.; Espinola, R.; Nogales, F.; Conejo, A. ARIMA models to predict next-day electricity prices. *IEEE Trans. Power Syst.* **2003**, *18*, 1014–1020. [[CrossRef](#)]
8. Georgescu, I.A.; Oprea, S.V.; Bâra, A. Time-frequency connectedness between electricity prices in Romania and its determinants in the competitive markets. *Kybernetes*, **2024**; *ahead-of-print*.
9. Kovalnogov, V.N.; Fedorov, R.V.; Chukalin, A.V.; Klyachkin, V.N.; Tabakov, V.P.; Demidov, D.A. Applied Machine Learning to Study the Movement of Air Masses in the Wind Farm Area. *Energies* **2024**, *17*, 3961. [[CrossRef](#)]
10. Hernández Rodríguez, M.; Baca Ruiz, L.G.; Criado Ramón, D.; Pegalajar Jiménez, M.D. Artificial Intelligence-Based Prediction of Spanish Energy Pricing and Its Impact on Electric Consumption. *Mach. Learn. Knowl. Extr.* **2023**, *5*, 431–447. [[CrossRef](#)]
11. López, G.; Arboleya, P. Short-term wind speed forecasting over complex terrain using linear regression models and multivariable LSTM and NARX networks in the Andes Mountains, Ecuador. *Renew. Energy* **2022**, *183*, 351–368. [[CrossRef](#)]
12. Veeramsetty, V.; Reddy, K.R.; Santhosh, M.; Mohnot, A.; Singal, G. Short-term electric power load forecasting using random forest and gated recurrent unit. *Electr. Eng.* **2022**, *104*, 307–329. [[CrossRef](#)]
13. Ordóñez, F.J.; Roggen, D. Deep convolutional and LSTM recurrent neural networks for multimodal wearable activity recognition. *Sensors* **2016**, *16*, 115. [[CrossRef](#)]

14. Wang, L.; Zhang, Z.; Chen, J. Short-term electricity price forecasting with stacked denoising autoencoders. *IEEE Trans. Power Syst.* **2016**, *32*, 2673–2681. [[CrossRef](#)]
15. Zhang, J.; Tan, Z.; Wei, Y. An adaptive hybrid model for short term electricity price forecasting. *Appl. Energy* **2020**, *258*, 114087. [[CrossRef](#)]
16. Yang, M.; Jiang, Y.; Che, J.; Han, Z.; Lv, Q. Short-Term Forecasting of Wind Power Based on Error Traceability and Numerical Weather Prediction Wind Speed Correction. *Electronics* **2024**, *13*, 1559. [[CrossRef](#)]
17. Loizidis, S.; Kyprianou, A.; Georgiou, G.E. Electricity market price forecasting using ELM and Bootstrap analysis: A case study of the German and Finnish Day-Ahead markets. *Appl. Energy* **2024**, *363*, 123058. [[CrossRef](#)]
18. Pourdaryaei, A.; Mohammadi, M.; Mubarak, H.; Abdellatif, A.; Karimi, M.; Gryazina, E.; Terzija, V. A new framework for electricity price forecasting via multi-head self-attention and CNN-based techniques in the competitive electricity market. *Expert Syst. Appl.* **2024**, *235*, 121207. [[CrossRef](#)]
19. Laitos, V.; Vontzos, G.; Bargiotas, D.; Daskalopulu, A.; Tsoukalas, L.H. Data-Driven Techniques for Short-Term Electricity Price Forecasting through Novel Deep Learning Approaches with Attention Mechanisms. *Energies* **2024**, *17*, 1625. [[CrossRef](#)]
20. Yang, W.; Sun, S.; Hao, Y.; Wang, S. A novel machine learning-based electricity price forecasting model based on optimal model selection strategy. *Energy* **2022**, *238*, 121989. [[CrossRef](#)]
21. Jaseena, K.U.; Kovoor, B.C. Decomposition-based hybrid wind speed forecasting model using deep bidirectional LSTM networks. *Energy Convers. Manag.* **2021**, *234*, 113944. [[CrossRef](#)]
22. Sulandari, W.; Lee, M.H.; Rodrigues, P.C. Indonesian electricity load forecasting using singular spectrum analysis, fuzzy systems and neural networks. *Energy* **2020**, *190*, 116408. [[CrossRef](#)]
23. Fu, Y.; Zhang, D.; Xiao, Y.; Wang, Z.; Zhou, H. An interpretable time series data prediction framework for severe accidents in nuclear power plants. *Entropy* **2023**, *25*, 1160. [[CrossRef](#)] [[PubMed](#)]
24. He, H.; Gao, S.; Jin, T.; Sato, S.; Zhang, X. A seasonal-trend decomposition-based dendritic neuron model for financial time series prediction. *Appl. Soft Comput.* **2021**, *108*, 107488. [[CrossRef](#)]
25. Zhang, X. Ion channel prediction using Lightgbm Model. In Proceedings of the 2020 International Conference on Big Data, Artificial Intelligence and Internet of Things Engineering (ICBAIE), Fuzhou, China, 12–14 June 2020; IEEE: New York, NY, USA, 2020; pp. 349–352.
26. Stefanon, S.F.; Seman, L.O.; Mariani, V.C.; Coelho, L.d.S. Aggregating prophet and seasonal trend decomposition for time series forecasting of Italian electricity spot prices. *Energies* **2023**, *16*, 1371. [[CrossRef](#)]
27. Wang, C.; Li, Y.; Wu, Q.; Wu, R. Research on Regional Short-term Load Forecasting Based on SVM-STL-LSTM. *Water Resour. Water Power* **2024**, *42*, 215–218.
28. Tan, M.; Hu, C.; Chen, J.; Wang, L.; Li, Z. Multi-node load forecasting based on multi-task learning with modal feature extraction. *Eng. Appl. Artif. Intell.* **2022**, *112*, 104856. [[CrossRef](#)]
29. Ke, G.; Meng, Q.; Finley, T.; Wang, T.; Chen, W.; Ma, W.; Ye, Q.; Liu, T.Y. Lightgbm: A highly efficient gradient boosting decision tree. *Adv. Neural Inf. Process. Syst.* **2017**, *30*, 3147–3155.
30. Duan, Y.; Chen, G.; Zhang, Y.; Jiang, C.; Guo, F.; Deng, S.; Yan, H. Day-ahead Price Forecast of Spot Market Based on LightGBM-IndRNN Model. *Water Power* **2023**, *49*, 84–87+93.
31. Wang, X.; Xu, N.; Meng, X.; Chang, H. Prediction of gas concentration based on LSTM-LightGBM variable weight combination model. *Energies* **2022**, *15*, 827. [[CrossRef](#)]
32. Lundberg, S.M.; Lee, S.I. A unified approach to interpreting model predictions. *Adv. Neural Inf. Process. Syst.* **2017**, *30*, 4768–4777.
33. Dash, G.; Paul, J. CB-SEM vs PLS-SEM methods for research in social sciences and technology forecasting. *Technol. Forecast. Soc. Change* **2021**, *173*, 121092. [[CrossRef](#)]
34. Wang, Y.; Deng, F.; Yang, X. A Hybrid Pork Price Forecast Model Based on LightGBM and Segment-wise Attention. In Proceedings of the ICCEIC, Chongqing, China, 25–27 November 2022; pp. 226–233.
35. Ozdemir, A.C.; Buluş, K.; Zor, K. Medium-to long-term nickel price forecasting using LSTM and GRU networks. *Resour. Policy* **2022**, *78*, 102906. [[CrossRef](#)]
36. Xia, M.; Shao, H.; Ma, X.; de Silva, C.W. A stacked GRU-RNN-based approach for predicting renewable energy and electricity load for smart grid operation. *IEEE Trans. Ind. Inform.* **2021**, *17*, 7050–7059. [[CrossRef](#)]

**Disclaimer/Publisher’s Note:** The statements, opinions and data contained in all publications are solely those of the individual author(s) and contributor(s) and not of MDPI and/or the editor(s). MDPI and/or the editor(s) disclaim responsibility for any injury to people or property resulting from any ideas, methods, instructions or products referred to in the content.